RSC Advances

PAPER

View Article Online
View Journal | View Issue



Cite this: *RSC Adv.*, 2022, **12**, 27970

# Norsesquiterpenoids from the octocoral *Paralemnalia thyrsoides* (Ehrenberg 1834)†

Gia Hung Phan,‡[ab] Hao-Chun Hu,‡[c] Fang-Rong Chang,[c] Zhi-Hong Wen,[de] Jih-Jung Chen,[f] Hsu-Ming Chung,[g] Yu-Chi Tsai*[h] and Ping-Jyun Sung*[bcdij]

Received 10th August 2022
Accepted 24th September 2022

DOI: 10.1039/d2ra05015c

rsc.li/rsc-advances

Three norsesquiterpenoids, pathyspirolactones A (**1**) and B (**2**), and napalilactone (**3**), featuring a γ-spirolactone moiety, were isolated from the cultured octocoral *Paralemnalia thyrsoides*. The structures of **1**–**3** were determined by analyzing spectroscopic data, DP4+ computation, specific optical rotation, and X-ray diffraction. In addition, we explored the absolute configurations of pathyspirolactone A (**1**) and its conformation of the cyclohexane ring to resolve the stereochemical confusion of those of norsesquiterpenoid compounds. Furthermore, we proved that pathyspirolactone B (**2**) was the first bromine-containing norsesquiterpenoid reported from octocorals.

## 1 Introduction

Octocorals of the genus *Paralemnalia* (family Nephtheidae) represent a rich source of natural substances with intriguing and unique structural features. Among these metabolites, sesquiterpenoids[1–10] and norsesquiterpenoids[11–14] are representative compounds for the natural products from *Paralemnalia* spp. *Paralemnalia thyrsoides* (Ehrenberg 1834) is one of the most common marine invertebrates natively distributed throughout tropical and subtropical regions of the Indo-Pacific Ocean. Corals were described by Shi-Zhen Li in his ancient herbal Compendium of Chinese Materia Medica, published in 1596, as "sweet, neutral and non-toxic; used to remove eye vision obstruction; clear abiding static blood; blow the powder to nose to stop nose bleeding; brighten the eye and calm the spirit; stop epileptic seizure; apply to the eye to improve floater."[15] In connection with our continuing studies of marine organisms with the aim of informing new natural products, in this research, we completed the preparation and structural identification of two nor-sesquiterpenoids, pathyspirolactones A (**1**) and B (**2**), and a known analogue, napalilactone (**3**) (Fig. 1), obtained from the cultured octocoral identified as *P. thyrsoides*.

## 2 Results and discussion

Pathyspirolactone A (**1**) was isolated as an amorphous powder. NMR data coupled with the $[M + Na]^+$ peak in the HRESIMS at *m*/*z* 277.14129 suggested a molecular formula $C_{14}H_{22}O_4$ (calcd for $C_{14}H_{22}O_4$ + Na, 277.14103) that indicated four degrees of unsaturation. IR spectrum analysis showed that **1** had absorption peaks at $\nu_{max}$ 3422, 1762, and 1700 $cm^{-1}$, suggesting that

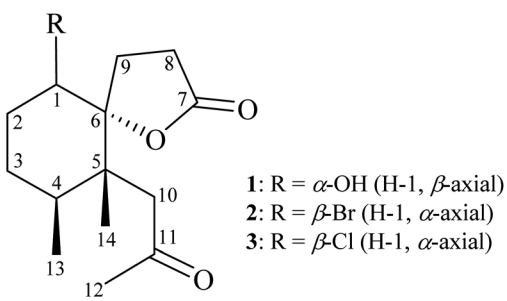


Fig. 1 Structures of pathyspirolactones A (**1**) and B (**2**), and napalilactone (**3**).

[a]*Graduate Institute of Marine Biology, National Dong Hwa University, Pingtung 944401, Taiwan*
[b]*National Museum of Marine Biology and Aquarium, Pingtung 944401, Taiwan. E-mail: pjsung@nmmba.gov.tw*
[c]*Graduate Institute of Natural Products, Kaohsiung Medical University, Kaohsiung 807378, Taiwan*
[d]*Department of Marine Biotechnology and Resources, National Sun Yat-sen University, Kaohsiung 804201, Taiwan*
[e]*Institute of BioPharmaceutical Sciences, National Sun Yat-sen University, Kaohsiung 804201, Taiwan*
[f]*Department of Pharmacy, School of Pharmaceutical Sciences, National Yang Ming Chiao Tung University, Taipei 112304, Taiwan*
[g]*Department of Applied Chemistry, National Pingtung University, Pingtung 900391, Taiwan*
[h]*School of Chinese Medicine, College of Chinese Medicine, China Medical University, Taichung 404328, Taiwan. E-mail: yuchi0713@gmail.com*
[i]*Chinese Medicine Research and Development Center, China Medical University Hospital, Taichung 404394, Taiwan*
[j]*PhD Program in Pharmaceutical Biotechnology, Fu Jen Catholic University, New Taipei City 242062, Taiwan*

† Electronic supplementary information (ESI) available: HRESI-MS, 1D and 2D-NMR spectra of **1** and **2**; ESI-MS and 1D-NMR spectra of **3**; experimental and calculated SOR values of **1** and **2**; X-ray crystallo-graphic data of **3**; DP4+ analysis of **1** and **2**. CCDC 2190441. For ESI and crystallographic data in CIF or other electronic format see https://doi.org/10.1039/d2ra05015c

‡ These authors have contributed equally to this work.

Table 1 $^{1}H$ and $^{13}C$ NMR spectroscopic data of pathyspirolactones A (**1**) and B (**2**), napalilactone (**3**), and *epi*-pathylactone

| | 1 | | 2 | | 3 | | *epi*-pathylactone | |
|---|---|---|---|---|---|---|---|---|
| Position | $\delta_H$[a] ($J$ in Hz) | $\delta_C$[b], Mult[c] | $\delta_H$[a] ($J$ in Hz) | $\delta_C$[b], Mult[c] | $\delta_H$[a] ($J$ in Hz) | $\delta_C$[b], Mult[c] | $\delta_H$[h] ($J$ in Hz) | $\delta_C$[h] |
| 1β$_{(axial)}$ | 3.70 dd (11.6, 4.8) | 73.4, CH | | | | | | |
| 1β$_{(equiv.)}$ | | | | | | | 4.27 m[i] | 65.0 |
| 1α$_{(axial)}$ | | | 4.59 dd (12.0, 4.4) | 58.2, CH | 4.36 dd (10.4, 4.4) | 63.8, CH | | |
| 2α$_{(axial)}$ | 1.63 m | 30.4, $CH_2$ | | | | | | |
| 2β$_{(equiv.)}$ | 1.81 m | | | | | | | |
| 2α$_{(equiv.)}$/β$_{(axial)}$ | | | 2.23 m; 2.08 ddd (14.4, 12.0, 4.0) | 29.8, $CH_2$ | 2.12 m; 1.94 m | 28.9, $CH_2$ | 1.78–2.0 | 27.0 |
| 3α$_{(equiv.)}$ | 1.61 m | 28.4, $CH_2$ | | | | | | |
| 3β$_{(axial)}$ | 1.41 m | | | | | | | |
| 3α$_{(axial)}$/β$_{(equiv.)}$ | | | 1.89 m; 1.45 dddd (14.0, 4.0, 4.0, 4.0) | 28.1, $CH_2$ | 1.83 m; 1.50 m | 27.0, $CH_2$ | 1.44–1.79 | 26.0 |
| 4 | 2.17 m | 34.3, CH | 2.56 m[d] | 33.2, CH | 2.53 m | 33.2, CH | 2.38 | 33.7 |
| 5 | | 46.7, C | | 46.4,[f] C | | 46.2, C | | 45.3 |
| 6 | | 91.8, C | | 91.1, C | | 91.5, C | | 92.0 |
| 7 | | 177.9, C | | 175.8, C | | 175.9, C | | 177.0 |
| 8 | 2.74 ddd (17.2, 12.4, 8.0); 2.47 ddd (17.2, 11.2, 4.2) | 29.6, $CH_2$ | 2.74 m[e]; 2.53 m[d] | 29.7, $CH_2$ | 2.68 m[g]; 2.46 m | 29.4, $CH_2$ | 2.48–2.67 | 29.0 |
| 9 | 2.37 m; 2.19 m | 26.3, $CH_2$ | 2.48 m; 2.41 m | 26.2, $CH_2$ | 2.39 d (10.0); 2.37 dd (10.0, 2.0) | 24.8, $CH_2$ | 2.30 | 24.0 |
| 10 | 2.47 s | 48.9, $CH_2$ | 2.89 d (16.0); 2.76 d (16.0[e]) | 46.4[f], $CH_2$ | 2.84 d (16.0); 2.70 d (16.0[g]) | 46.8, $CH_2$ | 2.80–2.73 (two doublet, $J$ = 15.1) | 47.0 |
| 11 | | 208.4, C | | 207.9, C | | 208.0, C | | 207.0 |
| 12 | 2.20 s | 32.3, $CH_3$ | 2.16 s | 33.0, $CH_3$ | 2.16 s | 32.9, $CH_3$ | 2.09 s | 32.2 |
| 13 | 0.99 d (7.2) | 16.6, $CH_3$ | 1.03 d (7.6) | 15.7, $CH_3$ | 1.01 d (7.6) | 15.7, $CH_3$ | 0.96 d (7.7) | 15.9 |
| 14 | 0.91 s | 15.0, $CH_3$ | 1.23 s | 18.6, $CH_3$ | 1.18 s | 18.0, $CH_3$ | 1.12, s | 17.2 |

[a] Spectra recorded at 400 MHz in $CDCl_3$. [b] Spectra recorded at 100 MHz in $CDCl_3$. [c] Multiplicity deduced by DEPT and HSQC spectra and indicated by usual symbols. [d] Signals overlapped. [e] Signals overlapped. [f] Signals overlapped. [g] Signals overlapped. [h] Data were reported by Coelho and Diaz.[16] These data were recorded at 500 MHz for $^{1}H$ and 125 MHz for $^{13}C$ in $CDCl_3$. [i] The coupling pattern and coupling constants were assigned as "two similar coupling constants ($J$ = 4.2, 2.9 Hz)" in the content text of the ref. 16.

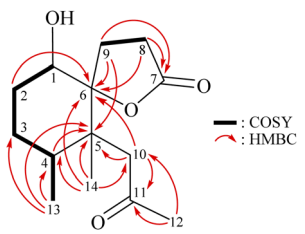


Fig. 2 Key COSY and HMBC correlations of **1**.

the structure of **1** included hydroxy, γ-lactone, and ketonic groups. The $^{13}C$ NMR and DEPT spectra revealed that compound **1** had 14 carbons (Table 1), including three methyls, five $sp^3$ methylenes, two $sp^3$ methines (including one oxymethine), two $sp^3$ quaternary carbons (including one oxygenated quaternary carbon), one ester carbonyl and one ketonic carbonyl carbon. Therefore, according to the aforementioned data, two degrees of unsaturation were accounted for, and compound **1** was identified as having two rings.

From the $^{1}H$–$^{1}H$ COSY spectrum (Fig. 2), the data suggested that it was possible to differentiate between the separate spin systems of H-1/$H_2$-2/$H_2$-3/H-4/$H_3$-13 and $H_2$-8/$H_2$-9. Together with the key HMBC correlations of **1**, such as H-4, $H_2$-9, $H_2$-10, $H_3$-13, $H_3$-14/C-5; $H_2$-2, H-8, H-9, $H_2$-10, $H_3$-14/C-6; $H_2$-8, $H_2$-9/C-7; and $H_2$-10, $H_3$-12/C-11, these data confirmed the main carbon skeleton of **1**. The HMBC correlations from $H_3$-12/C-10, C-11; $H_3$-13/C-3, C-4, C-5; and $H_3$-14/C-4, C-5, C-6, C-10 indicated that $CH_3$-12, $CH_3$-13, and $CH_3$-14 were placed at C-11, C-4, and C-5, respectively (Fig. 2).

The relative stereochemistry of **1** was deduced mainly from the NOE interactions in the NOESY experiment, Chem3D

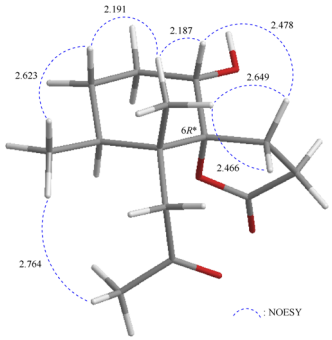


Fig. 3 Stereo-view of **1** (generated by computer modeling) and calculated distances (Å) between selected protons with key NOESY correlations.

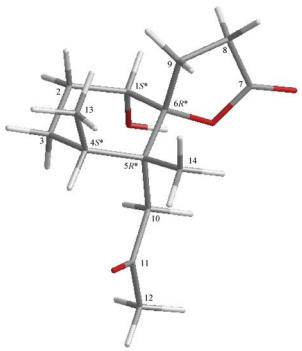

Fig. 4 Stereo-view of *epi*-pathylactone A (generated by computer modeling).

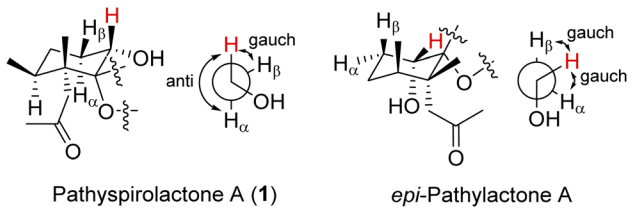


Fig. 5 Newman projection of H-1 in **1** and *epi*-pathylactone A.

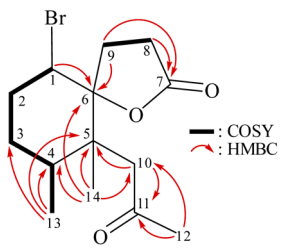


Fig. 6 Key COSY and HMBC correlations of **2**.

Model, and vicinal $^{1}H$–$^{1}H$ coupling constant analysis. In accordance with convention, when analyzing the stereochemistry of **1**, the tertiary C-14 methyl group at C-5 was assigned to the β-face, anchoring stereochemical analysis. In the NOESY experiment (Fig. 3), the correlations of $H_3$-14 with H-1 and $H_2$-9 showed that these protons were positioned on the same face of the molecule, and therefore they were assigned as β-protons. One of the methylene protons at C-3 ($\delta_H$ 1.41) exhibited a correlation with $H_3$-14, leading to its assignment as H-3β, while the other was denoted as H-3α ($\delta_H$ 1.61). The correlation between H-3β and $H_3$-13 reflected the β-orientation of the $CH_3$-13 group at C-4. The configuration at the cyclohexane ring in **1** is worthy of comment. H-1 was found to exhibit correlations with $H_3$-14, as well as coupling between H-1 and $H_2$-2 ($J$ = 11.6, 4.8 Hz), indicating that both H-1 and C-14 methyl at C-5 should be oriented at β-axial positions. Therefore, based on the above findings, the configurations of the stereogenic carbons of **1** were determined as (1*S**, 4*S**, 5*R**, 6*R**).

It is very interesting to note that the structure of **1** as we presented herein had been reported and named *epi*-pathylactone A, a synthetic product by Coelho and Diaz in 2002.[16] Although these two compounds possessed the same relative configurations (1*S**, 4*S**, 5*R**, 6*S**) (Fig. 3 and 4), the different chemical shifts and coupling constants of H-1 in **1** ($\delta_H$ 3.70, 1H, dd, $J$ = 11.6, 4.8 Hz) and *epi*-pathylactone A ($\delta_H$ 4.27, 1H, $J$ = 4.2, 2.9 Hz)[16] demonstrated that H-1 had significantly different dihedral angles with H-2α and H-2β in both compounds, respectively. Furthermore, the $^{1}H$-NMR spectra of compound **1** at temperatures of 0, 25, and 50 °C were also measured to discover the $^{1}H$ chemical shift changes in those spectra. However, the critical proton NMR signal on C-1 ($\delta_H$ 3.70) in the different temperature experiments was quite similar (Fig. S27–S29†). Therefore, compound **1** was proposed as a new conformational isomer and did not undergo conformational interconversion after heat.

Based on the Newman projection analysis, H-1 in **1** expressed *anti* with H-2α and *gauch* with H-2β; H-1 in *epi*-pathylactone A showed *gauch* with the methylene protons on C-2 (Fig. 5), indicating H-1 should be in a β-axial position in **1** and β-equatorial in *epi*-pathylactone A. In addition, the conformational variation in the cyclohexane ring led to the structural difference in those compounds, resulting in the absolute configuration of **1** being hard to discuss by the reference comparison.

For solving the absolute stereochemistry issue of compound **1**, the DP4+ analysis was selective for double-checking the configuration of position C-1, which was the most confusing location for the type of compounds. The structures of **1**-1*S**, 4*S**, 5*R**, 6*R** (diastereomer 1) and **1**-1*R**, 4*S**, 5*R**, 6*R** (diastereomer 2) were computed GIAO-NMR data by Gaussian 09, and the calculated results were analysis by DP4+ (Fig. S11†). The DP4+ analysis results of **1**-1*S**, 4*S**, 5*R**, 6*R** displayed the match ratio 99.94%, 99.98%, and 100.00% in sDP4+ (all data), uDP4+ (all data), and DP4+ (all data), respectively (Table S1†). Furthermore, the possible configurations of **1**-1*S*, 4*S*, 5*R*, 6*R* and **1**-1*R*, 4*R*, 5*S*, 6*S* were input into spartan'16 and Gaussian 09 software for calculating conformational search, structure optimization, and specific optical rotation (SOR) value. As a result, the calculated SOR value of **1**-1*S*, 4*S*, 5*R*, 6*R* (66) was consistent with the experiment result of **1** (positive) (Table S2†). This is the first to clarify the absolute configuration of these

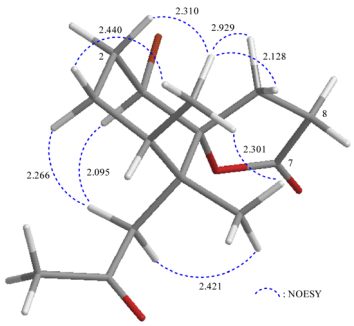


Fig. 7 Stereo-view of **2** (generated by computer modeling) and calculated distances (Å) between selected protons with key NOESY correlations.

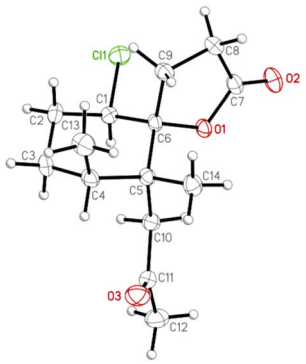


Fig. 8 The computer-generated ORTEP diagram of **3**.

norsesquiterpenoid -type compounds by *in silico* method and expounded on the differences in 1D-NMR data of the cyclohexane ring conformational variants.

Pathyspirolactone B (**2**) was isolated as an amorphous powder. ESIMS showed a pair of ion peaks at *m*/*z* 339/341 ($[M + Na]^+/[M + 2 + Na]^+$) (1 : 1), with the relative intensity indicative of a bromide substituent. NMR data coupled with the $[M + Na]^+$ peak in HRESIMS at *m*/*z* 339.05646 suggested a molecular formula $C_{14}H_{21}BrO_3$ (calcd for $C_{14}H_{21}BrO_3$ + Na, 339.05663), which indicated four degrees of unsaturation. IR absorptions at $\nu_{max}$ 1777 and 1712 $cm^{-1}$ suggested the presence of γ-lactone and ketonic groups. From the $^1H$ and $^{13}C$ NMR spectroscopic data, in combination with the DEPT spectrum (Table 1), two carbonyl resonances at $\delta_C$ 207.9 and 175.7 confirmed the presence of ketonic and γ-lactone moieties. So, from the NMR data, two degrees of unsaturation were accounted for, and **2** must be a bicyclic compound.

Due to electronegativity effects, the methine unit at $\delta_C$ 58.2 was more shielded than expected for oxygenated carbon and was correlated to the methine proton at $\delta_H$ 4.59 in the HSQC spectrum, proving the attachment of a bromide atom at C-1. These data, together with the $^1H$–$^1H$ COSY and HMBC correlations, established the molecular framework of **2** (Fig. 6). The NMR data of **2** were found to be close to those of a known halogenated norsesquiterpenoid, napalilactone (**3**),[17] which was also isolated in this study (Fig. 1), except for replacing a chlorine atom at C-1 in **3** ($\delta_H$ 4.36, 1H, dd, $J$ = 10.4, 4.4 Hz/$\delta_C$ 63.8, CH-1) (Fig. S25 and S26†) with a bromine atom in **2** ($\delta_H$ 4.59, 1H, dd, $J$ = 12.0, 4.4 Hz 4.0 Hz/$\delta_C$ 58.2, CH-1). To the best of our knowledge, compound **2** is the first bromine-containing norsesquiterpenoid reported from octocorals.

The relative configuration of **2** was elucidated from the interactions observed in a NOESY experiment. Furthermore, it was found to be compatible with that of **2** offered by computer modeling (Fig. 7) and that obtained from vicinal proton coupling constant analysis. In the NOESY spectrum of **2**, H-1 showed a correlation with one proton of $CH_2$-10 ($\delta_H$ 2.76) and a large coupling constant with H-2β ($J$ = 12.0 Hz), indicating an α-axial orientation of H-1. The methyl proton $H_3$-14 exhibited correlations with $H_3$-13 and $H_2$-9 but without $H_2$-10, revealing the β-orientations of Me-13, Me-14, and C-9 methylene at C-4, C-5, and C-7, respectively. Moreover, **2**-1*R**, 4*S**, 5*R**, 6*R** (diastereomer 1) and **2**-1*S**, 4*S**, 5*R**, 6*R** (diastereomer 2) were further submitted into Gaussian 09 for computed GIAO-NMR data for DP4+ analysis. The analysis results of 2-1*R**, 4*S**, 5*R**, 6*R** exhibited a 100% matched ratio with the experimental data of **2** in sDP4+ (all data), uDP4+ (all data), and DP4+ (all data) (Table S1†). Consequently, the relative configuration of **2** was elucidated to be 1*R**, 4*S**, 5*R**, 6*R**.

Furthermore, the SOR was used for determining the absolute configuration of 2. The calculated SOR of 2-1*R*, 4*S*, 5*R*, 6*R* and 2-1*S*, 4*R*, 5*S*, 6*S* exhibited a positive (12) and a negative (−12) value, respectively (Table S1†). The experiment SOR data of **2** (positive) was matched with the 2-1*R*, 4*S*, 5*R*, 6*R*. However, as the similar issue of **1**, the absolute configuration of C-1 cast doubt on **2**.

Moreover, the absolute configuration of napalilactone (**3**) was fully established by a single-crystal X-ray diffraction analysis with the Flack parameter $x = -0.04(4)$.[18,19] The computer-generated ORTEP diagram (Fig. 8) showed the absolute configuration of stereogenic centers of **3** were 1*R*, 4*S*, 5*R*, 6*R*. Based on the principles of biogenetics and the above DP4+ analysis, pathyspirolactone B (**2**) can be verified as the same absolute configuration as **3**.

Based on the past reports, *Paralemnalia* spp. showed a promising anti-inflammatory effect and cytotoxic activity.[7,8,10,14] Therefore, in *in vitro* anti-inflammatory activity tests, upregulation of pro-inflammatory inducible nitric oxide synthase (iNOS) and cyclooxygenase-2 (COX-2) protein expression in LPS-stimulated RAW 264.7 macrophage cells were evaluated using immunoblot analysis. At a concentration of 10 μM, norsesquiterpenoids **1** and **2** were found to be inactive to reduce the level of iNOS and COX-2 in relation to control cells stimulated with LPS only. Using trypan blue staining to measure the cytotoxic effects of the compounds, it was observed that **1** and **2** did not induce cytotoxicity in RAW 264.7 macrophage cells.

## 3 Conclusions

In summary, we obtained three norsesquiterpenoids, including pathyspirolactones A (**1**) and B (**2**), and napalilactone (**3**) from octocoral *P. thyrsoides*. We further explored the conformation of

the cyclohexane ring moiety to resolve the stereochemical confusion of those of norsesquiterpenoid compounds. Moreover, we demonstrated the absolute configurations of pathyspirolactones based on analyzing spectroscopic data, specific optical rotation, DP4+ computation, and X-ray diffraction. However, because the screening platforms were limited and lots of material were consumed in physical and spectral experiments, the other possible bioactivities for the new interesting natural substances will not be assayed at this stage.

# 4 Experimental

## 4.1 General experimental procedures

Optical rotation values were measured using a JASCO P-1010 digital polarimeter. IR spectra were obtained with a Thermo Scientific Nicolet iS5 FT-IR spectrophotometer. NMR spectra were recorded on a 400 MHz Jeol ECZ NMR spectrometer using the residual $CHCl_3$ ($\delta_H$ 7.26 ppm) and $CDCl_3$ signals ($\delta_C$ 77.0 ppm) as internal standards for $^1H$ and $^{13}C$ NMR, respectively; coupling constants ($J$) are presented in Hz. ESIMS and HRESIMS were recorded using a Bruker 7 Tesla solariX FTMS system. Column chromatography was carried out with silica gel (230–400 mesh, Merck). TLC was performed on plates precoated with silica gel 60 $F_{254}$ (Merck) and RP-18W/$UV_{254}$ (0.15 mm-thick, Macherey-Nagel), then sprayed with 20% $H_2SO_4$ solution followed by heating to visualize the spots. NP-HPLC was performed using a system comprised of a Hitachi L-5110 pump and a Rheodyne 7725i injection port with a normal-phase column (Galaksil® EF-$SiO_2$, 5 μm 120 Å, S/N E08210401; Galak Co., Wuxi, CN). RP-HPLC was performed using a system comprised of a Hitachi L-2130 pump, a Hitachi L-2455 photodiode array detector, and a Rheodyne 7725i injection port with a reverse-phase column (Supelco, Ascentis® C18, 581343-U, 250 mm × 10 mm, 5 μm).

## 4.2 Animal material

Specimens of *Paralemnalia thyrsoides* (Ehrenberg, 1834) used for this study were collected from the culturing tank in the NMMBA in June 2021. A voucher specimen was deposited in the NMMBA (voucher no.: NMMBA-TW-SC-2021-902). Identification of the species of this organism was performed by comparison as described in previous studies.[20–22]

## 4.3 Extraction and isolation

The freeze-dried and sliced bodies of the coral specimen (wet/dry weight = 2031/299 g) were extracted by 95% EtOH to yield a crude extract I (31.7 g) and continued to be extracted by the mixture of MeOH/$CH_2Cl_2$ (1 : 1) to give an extract II (29.5 g). Then extracts I and II were partitioned with EtOAc and $H_2O$ to obtain the EtOAc-soluble layers A (8.9 g) and B (1.8 g), respectively. The EtOAc layers A and B were then combined, placed in a silica column, and eluted by hexanes/EtOAc (pure hexanes to pure EtOAc, stepwise) to yield ten fractions A–J. Fraction G (121.3 mg) was further separated by normal-phase HPLC on Galaksil® EF-$SiO_2$ column with a mixture of *n*-hexane and acetone (65 : 35) at a rate of 5 mL $min^{-1}$ to give four subfractions ($G_1$–4). $G_2$ (63.2 mg) was subjected to the normal-phase HPLC system with an isocratic solvent system of *n*-hexane and ethyl acetate (80 : 20, 5 mL $min^{-1}$) to yield 12 fractions ($G_2A$–L). $G_2L$ (48.6 mg) was then separated by the normal-phase HPLC system using a mixture of *n*-hexane and acetone (80 : 20, 5 mL $min^{-1}$) to obtain 15 subfractions (G2L1–15). G2L10 (10.9 mg) was further purified by reverse-phase HPLC on Ascentis® C18 column with an isocratic solvent system of MeOH and $H_2O$ (55 : 45, 5 mL $min^{-1}$) to obtain compound **1** (0.2 mg). Fraction D (710.1 mg) was subjected to the normal-phase HPLC system with a mixture of *n*-hexane and ethyl acetate (85 : 15, 5 mL $min^{-1}$) to give nine subfractions (D1–9). D7 (18.2 mg) was further purified by the reverse-phase HPLC using a mixture solvent system of MeOH : $H_2O$ (50 : 50, 5 mL $min^{-1}$) to obtain compounds **2** (0.3 mg) and **3** (11.6 mg).

## 4.4 Structural characterization of undescribed compounds

**4.4.1 Pathyspirolactone A (1).** Amorphous powder; [$\alpha$] +185 (*c* 0.01, $CHCl_3$); IR (ATR) $\nu_{max}$ 3422, 1762, 1700 $cm^{-1}$; $^1H$ (400 MHz, $CDCl_3$) and $^{13}C$ (100 MHz, $CDCl_3$) NMR data (see Table 1); ESIMS: *m*/*z* 277 $[M + Na]^+$; HRESIMS *m*/*z* 277.14129 (calcd for $C_{14}H_{22}O_4$ + Na, 277.14103).

**4.4.2 Pathyspirolactone B (2).** Amorphous powder; [$\alpha$] +44 (*c* 0.01, $CHCl_3$); IR (ATR) $\nu_{max}$ 1777, 1712 $cm^{-1}$; $^1H$ (400 MHz, $CDCl_3$) and $^{13}C$ (100 MHz, $CDCl_3$) NMR data (see Table 1); ESIMS: *m*/*z* 339 $[M + Na]^+$, 341 $[M + 2 + Na]^+$; HRESIMS *m*/*z* 339.05646 (calcd for $C_{14}H_{21}BrO_3$ + Na, 339.05663).

**4.4.3 Napalilactone (3).** Colorless crystal ($CDCl_3$); [$\alpha$] +46 (*c* 0.58, $CHCl_3$); $^1H$ (400 MHz, $CDCl_3$) and $^{13}C$ (100 MHz, $CDCl_3$) NMR spectra please see the ESI Fig. S25 and S26;† ESIMS: *m*/*z* 295 $[M + Na]^+$, 297 $[M + 2 + Na]^+$ ($C_{14}H_{21}ClO_3$ + Na).

## 4.5 Single-crystal X-ray crystallography of napalilactone (3)

Suitable colorless prisms of napalilactone (**3**) were obtained from $CDCl_3$. The crystal (0.599 × 0.512 × 0.081 $mm^3$) was identified as being of the orthorhombic system, space group $P2_12_12_1$ (#19), with $a$ = 8.2367(2) Å, $b$ = 9.9002(3) Å, $c$ = 17.2237(5) Å, $V$ = 1404.51(7) $Å^3$, $Z$ = 4, $D_{calcd}$ = 1.290 Mg $m^{-3}$, $\lambda$ (Mo K$\alpha$) = 0.71073 Å. Intensity data were obtained on a crystal diffractometer (Bruker, model: D8 Venture) up to $\theta_{max}$ of 30.0°. All measurement data of 39 483 reflections were collected, of which 4100 were independent. The structure was solved by direct methods and refined by a full-matrix least-squares on the $F^2$ procedure.[23] The refined structural model converged to a final $R_1$ = 0.0460; $wR_2$ = 0.1060 for 3494 observed reflections [$I > 2\sigma(I)$] and 172 variable parameters; and the absolute configuration was determined from the Flack parameter $x$ = −0.04(4).[18,19] Crystallographic data for the structure of napalilactone (**3**) were submitted to the Cambridge Crystallographic Data Center (CCDC) with supplementary publication number CCDC 2190441 (data can be obtained from the CCDC website at https://www.ccdc.cam.ac.uk/conts/retrieving.html).

## 4.6 *In silico* calculations

The structure was optimized the minimized energy in MM2 level and outputted as an xyz file. The file was submitted into

spartan'16 software (Wavefunction Inc.; Irvine, CA, USA) at MMFF94 to generate conformational search results. The output data were imported into the Gaussian 09 software (Gaussian Inc.; Wallingford, CT, USA) and optimized using the time-dependent density functional theory (TDDFT) methodology at the B3LYP/6-31G* level in the gas phase, and at the B3LYP/6-31(d) levels in the solvent phase for SOR calculation, and the GIAO-DFT at the PCM/mpw1pw91/6-311 + g(d,p) level in the solvent phase for GIAO-NMR DP4+ analysis. All the computed SOR and NMR results were averaged by the proportion of each conformer.[24,25]

## Conflicts of interest

There are no conflicts to declare.

## Acknowledgements

The authors are grateful to Hsiao-Ching Yu and Chao-Lien Ho of the High Valued Instrument Center, National Sun Yat-sen University, for obtaining the mass (MS000600) and NMR (NMR 001100) spectra (MOST 111-2731-M-110-001). This work was mainly funded by grants from the National Museum of Marine Biology and Aquarium and the National Science and Technology Council (MOST 109-2320-B-291-001-MY3 and 111-2320-B-291-001 (1/3)), Taiwan, awarded to P.-J. S. All funding is gratefully acknowledged.

## Notes and references

1 D. Daloze, J. C. Braekman, P. Georget and B. Tursch, Chemical studies of marine invertebrates. XXII. (1) Two novel sesquiterpenes from soft corals of the genera *Lemnalia* and *Paralemnalia* (Coelenterata, Octocorallia, Alcyonacea), *Bull. Soc. Chim. Belg.*, 1977, **86**, 47–54.

2 B. F. Bowden, J. C. Coll and S. J. Mitchell, Studies of Australian soft corals. XIX. Two new sesquiterpenes with the nardosinane skeleton from a *Paralemnalia* species, *Aust. J. Chem.*, 1980, **33**, 885–890.

3 J. Y. Su, Y. L. Zhong and L. M. Zeng, Two new sesquiterpenoids from the soft coral *Paralemnalia thyrsoides*, *J. Nat. Prod.*, 1993, **56**, 288–291.

4 H. C. Huang, C. H. Chao, J. H. Su, C. H. Hsu, S. P. Chen, Y. H. Kuo and J. H. Sheu, Neolemnane-type sesquiterpenoids from a Formosan soft coral *Paralemnalia thyrsoides*, *Chem. Pharm. Bull.*, 2007, **55**, 876–880.

5 A. Bishara, D. Yeffet, M. Sisso, G. Shmul, M. Schleyer, Y. Benayahu, A. Rudi and Y. Kashman, Nardosinanols A–I and lemnafricanol, sesquiterpenes from several soft corals, *Lemnalia* sp., *Paralemnalia clavata, Lemnalia africana*, and *Rhytisma fulvum fulvum*, *J. Nat. Prod.*, 2008, **71**, 375–380.

6 G. H. Wang, H. C. Huang, J. H. Su, Y. C. Wu, J. H. Sheu and J. -P. Paralemnolins, new sesquiterpenoids from the soft coral *Paralemnalia thyrsoide*, *Chem. Pharm. Bull.*, 2010, **58**, 30–33.

7 C. Y. Huang, J. H. Su, B. W. Chen, Z. H. Wen, C. H. Hsu, C. F. Dai, J. H. Sheu and P. J. Sung, Nardosinane-type sesquiterpenoids from the Formosan soft coral *Paralemnalia thyrsoides*, *Mar. Drugs*, 2011, **9**, 1543–1553.

8 Y. J. Tseng, Y. S. Lee, S. K. Wang, J. H. Sheu, C. Y. Duh and A. -D. Parathyrsoidins, four new sesquiterpenoids from the soft coral *Paralemnalia thyrsoides*, *Mar. Drugs*, 2013, **11**, 2501–2509.

9 X. Han, Q. Wang, X. Luo, X. Tang, Z. Wang, D. Zhang, S. Cao, P. Li, G. Li and A. -C. Lemnalemnanes, three rare rearranged sesquiterpenoids from the soft corals *Paralemnalia thyrsoides* and *Lemnalia* sp, *Org. Lett.*, 2022, **24**, 11–15.

10 A. Alassass, M. Abubakr, W. Alarif, S. E. Ayyad and A. E. Mohammed, Anti-inflammatory, antioxidant, cytotoxic activities, and sesquiterpenoid contents of *Paralemnalia thyrsoides*, *Pharmacogn. Mag.*, 2022, **18**, 188–192.

11 H. C. Huang, C. H. Chao, J. H. Liao, M. Y. Chiang, C. F. Dai, Y. C. Wu and J. H. Sheu, A novel chlorinated norsesquiterpenoid and two related new metabolites from the soft coral *Paralemnalia thyrsoides*, *Tetrahedron Lett.*, 2005, **46**, 7711–7714.

12 R. R. Izac, P. Schneider, M. Swain and W. Fenical, New nor-sesquiterpenoids of apparent nardosinane origin from the pacific soft-coral *Paralemnalia thyrsoides*, *Tetrahedron Lett.*, 1982, **23**, 817–820.

13 J. Y. Su, Y. L. Zhong, J. Q. Wu and L. M. Zeng, A new nor-sesquiterpenoid from the soft coral *Paralemnalia thyrsoids*, *Chin. Chem. Lett.*, 1991, **2**, 785–786.

14 Z. J. Zhang, W. F. Chen, B. R. Peng, Z. H. Wen and P. J. Sung, (+)-Pathylactone A, a new natural norsesquiterpenoid from the octocoral *Paralemnalia thyrsoides*, *Nat. Prod. Commun.*, 2018, **13**, 5–7.

15 Y. C. Chang, C. C. Chiang, Y. S. Chang, J. J. Chen, W. H. Wang, L. S. Fang, H. M. Chung, T. L. Hwang and P. J. Sung, Novel caryophyllane-related sesquiterpenoids with anti-inflammatory activity from *Rumphella antipathes* (Linnaeus, 1758), *Mar. Drugs*, 2020, **18**, 554.

16 F. Coelho and G. Diaz, Studies on the synthesis of (±)-pathylactone A, a norsesquiterpene lactone isolated from marine sources, *Tetrahedron*, 2002, **58**, 1647–1656.

17 J. R. Carney, A. T. Pham, W. Y. Yoshida and P. J. Scheuer, Napalilactone, a new halogenated norsesquiterpenoid from the soft coral *Lemnalia africana*, *Tetrahedron Lett.*, 1992, **33**, 7115–7118.

18 H. D. Flack, On enantiomorph-polarity estimation, *Acta Crystallogr.*, 1983, **A39**, 876–881.

19 H. D. Flack and G. Bernardinelli, Absolute structure and absolute configuration, *Acta Crystallogr.*, 1999, **A55**, 908–915.

20 C. F. Dai and C. H. Chin, *Octocorallia Fauna of Kenting National Park. Kenting National Park Headquarters: Kenting*, Pingtung, Taiwan, 2019, pp. 344–345.

21 C. F. Dai, *Ocean Center*, National Taiwan University, Taipei, Taiwan, 2021, pp. 436–437.Octocorallia Fauna of Taiwan.

22 C. F. Dai, *Corals of Taiwan: Octocorallia*, Owl Publishing House Co. Ltd., Taipei, Taiwan, 2022, 2, p. 267.

23 G. M. Sheldrick, SHELXT - Integrated space-group and crystal-structure determination, *Acta Crystallogr.*, 2015, **A71**, 3–8.

24 N. Grimblat, M. M. Zanardi and A. M. Sarotti, Beyond DP4: an improved probability for the stereochemical assignment of isomeric compounds using quantum chemical calculations of NMR shifts, *J. Org. Chem.*, 2015, **80**, 12526–12534.

25 H. C. Hu, Y. H. Tsai, Y. C. Chuang, K. H. Lai, Y. M. Hsu, T. L. Hwang, C. C. Lin, F. Fülöp, Y. C. Wu, S. Y. Yu, Y. T. Kuo and F. R. Chang, Estrogenic and anti-neutrophilic inflammatory phenanthrenes from *Juncus effusus* L, *Nat. Prod. Res.*, 2022, **36**, 3043–3053.